

## Period doubling and hysteresis in a periodically forced, damped anharmonic oscillator

M. Debnath and A. Roy Chowdhury

*High Energy Physics Division, Department of Physics, Jadavpur University, Calcutta 700 032, India*

(Received 27 August 1990)

The motion of a periodically forced, damped anharmonic oscillator governed by the equation of motion,  $\ddot{x} + v\dot{x} = A_2x + A_4x^3 + A_6x^5 + F \cos(\Omega t)$ , has been studied. The analysis of the response function of this equation when treated analytically, and later, numerically, uncovers a hysteresis-type phenomenon. The stability and response of the system and the onset of period doubling have been observed through an analytical approach, and they are corroborated with a numerical analysis for different values of  $F$  and  $\Omega$  ( $\Omega$  is the frequency of the periodic forcing system). Two different methods have been used. In the first, the damped system is converted into an undamped one by making an ansatz for  $\dot{x}$  of the form  $\dot{x} = R(x)$ , a polynomial in  $x$ . The second approach, however, studies the system directly. It has been observed that there exists a wide difference between these two systems. Furthermore, period doubling may be predicted through the use of the harmonic balance technique and Mathieu equation. Lastly, a numerical integration in phase space clearly indicates orbits corresponding to the initial period, then to double the initial period, and subsequently to higher multiples.

### I. INTRODUCTION

The steady-state vibrations in a nonlinear system under the influence of a periodic or quasiperiodic forcing term have been widely discussed.<sup>1</sup> The behavior of such systems is usually studied by appropriate analytical and numerical methods.<sup>2</sup> Such analysis reveals the existence of phenomena (such as subultra- or principal resonances, jump phenomena, or hysteresis) and a transition from a stable to an unstable region.<sup>3</sup> With the advent of the study of chaotic motion by means of strange attractors and Poincaré maps, it has become necessary to look for a better understanding of these nonlinear systems with higher-order nonlinear terms.

The present analysis has attempted to proceed through two different routes. In the first, the system is made to resemble an undamped one by making an ansatz for  $\dot{x}$ , that is, one sets  $\dot{x} = R(x)$ , where  $R$  is a polynomial in  $x$  and the consistency is forced (in the system without the forcing term). Such a method had been used<sup>4</sup> to obtain the heteroclinic orbits of the anharmonic system itself. In the second procedure, the damped system is treated directly. The analysis presented shows widely different characteristics of the two treatments attempted. The method of harmonic balance is used to study the skeleton<sup>3,5</sup> curve and the full resonance curves in both the situations. Then, the stability is analyzed by searching for the existence of stable nodes, foci, saddle points, etc. Lastly, the important phenomena of period doubling have been observed for different values of the parameters and the frequency of the periodic forcing system,  $\Omega$ , through a Mathieu-equation analysis.

The concluding part of the paper reports a numerical analysis of the equation in phase space by using the Runge-Kutta method. The results of the study confirm the period doubling observed in the analytical treatment

and show clearly the orbits corresponding to the initial time period  $T$ , and also for  $2T$ , and subsequently, for  $nT$ . Prior to achieving these results, the nature of the fixed points of the unperturbed system has also been exhibited.

### II. FORMULATION

#### A. Stability

##### 1. With the assumption of $\dot{x} = R(x)$

The nonlinear system under consideration has been presented as

$$\ddot{x} + v\dot{x} = P(x) + F \cos(\Omega t), \quad (1)$$

where  $P(x) = A_2x + A_4x^3 + A_6x^5$ . For  $F=0$ , Eq. (1) had been studied by Otwinowski, Paul, and Laidlaw.<sup>4</sup> They had shown that it was possible to obtain exact heteroclinic orbits, however, on the basis of the assumption  $\dot{x} = R(x) = a_2x + a_6x^3$ . This part of the present paper proceeds with the same assumption, and thus Eq. (1) may be written as

$$\ddot{x} + (va_6 - A_4)x^3 + (va_2 - A_2)x - A_6x^5 = F \cos(\Omega t). \quad (2)$$

Let  $k = va_6 - A_4$ ,  $\omega_0^2 = va_2 - A_2$ . Near the resonance,  $\Omega \approx \omega_0$ ; thus we set  $\Omega = \omega_0 + \epsilon\Delta$ . The strategy usually adopted is now followed, and thus it is assumed that

$$\begin{aligned} x &\approx a(t) \cos(\Omega t) + b(t) \sin(\Omega t) \\ &= r(t) \cos[\Omega t + \phi(t)]. \end{aligned} \quad (3)$$

Substituting in (2) and neglecting the higher harmonics the following may be arrived at:

$$-2\dot{a}\Omega + \epsilon\frac{3}{4}kb(a^2 + b^2) - \epsilon\frac{5}{8}A_6b(a^2 + b^2)^2 + (\omega_0^2 - \Omega^2)b = 0, \tag{4}$$

$$2\dot{b}\Omega + \epsilon\frac{3}{4}ka(a^2 + b^2) - \epsilon\frac{5}{8}A_6a(a^2 + b^2)^2 + (\omega_0^2 - \Omega^2)a = F.$$

Now using  $\omega_0^2 - \Omega^2 \approx -\epsilon(2\Omega) + O(\epsilon^2)$ , the following equations are obtained for the singular points  $(a_0, b_0)$  of (4):

$$\begin{aligned} \frac{3}{4}ka_0r_0^2 - \frac{5}{8}A_6a_0r_0^4 - 2\Omega\Delta a_0 &= \frac{F}{\epsilon} = F', \\ \frac{3}{4}kb_0r_0^2 - \frac{5}{8}A_6b_0r_0^4 - 2\Omega\Delta b_0 &= 0, \\ r_0^2 &= a_0^2 + b_0^2 = \rho. \end{aligned} \tag{5}$$

Equation (5) immediately leads to

$$\begin{aligned} \frac{25}{64}A_6^2\rho^5 - \frac{15}{16}k\rho^4 + \left[\frac{9}{16}k^2 + \frac{5}{4}A_6(2\Omega\Delta)\right]\rho^3 - \frac{3}{2}k(2\Omega\Delta)\rho^2 \\ + (2\Omega\Delta)^2\rho = \left[\frac{F}{\epsilon}\right]^2 = F'^2. \end{aligned} \tag{6}$$

The stability of the system can be studied by a small shift from the singular position  $(a_0, b_0)$ . We set  $a = a_0 + \alpha$ ,  $b = b_0 + \beta$  in Eq. (4). The Jacobian of the system is

$$\begin{bmatrix} C & D \\ A & B \end{bmatrix} = \begin{bmatrix} 0 & D \\ A & 0 \end{bmatrix}$$

and  $b_0 = 0$ , where

$$\begin{aligned} A &= \frac{1}{2\Omega} \left[ \frac{3}{4}ka_0^2 - \frac{5}{8}A_6a_0^4 - (2\Omega\Delta) \right], \\ D &= \frac{1}{2\Omega} \left[ -\frac{3}{4}k(3a_0^2) + \frac{25}{8}A_6a_0^4 + (2\Omega\Delta) \right]. \end{aligned} \tag{7}$$

Thus we have, as the condition for center,

$$AD < 0 \text{ as } B = C = 0,$$

which results in

$$\begin{aligned} \sigma = \left\{ \frac{125}{64}A_6^2\rho^4 - \frac{15}{4}kA_6\rho^3 + 3\left[\frac{9}{16}k^2 + \frac{5}{4}(2\Omega\Delta)A_6\right]\rho^2 \right. \\ \left. - 3k(2\Omega\Delta)\rho + (2\Omega\Delta)^2 \right\} > 0. \end{aligned} \tag{8}$$

The condition for saddle point is

$$AD > 0 \text{ as } B = C = 0,$$

which results in

$$\sigma < 0.$$

So the nature of the singular point may be ascertained by the curves  $\sigma = 0$  and Eq. (6).

In Fig. 1 we have plotted  $(2\Omega\Delta)$  versus  $\rho$  according to the equation  $\sigma = 0$  and Eq. (6) for various values of  $F'^2$ . The different types of region may occur depending upon the chosen parameter values. A few possible cases have been considered and shown in Fig. 1.

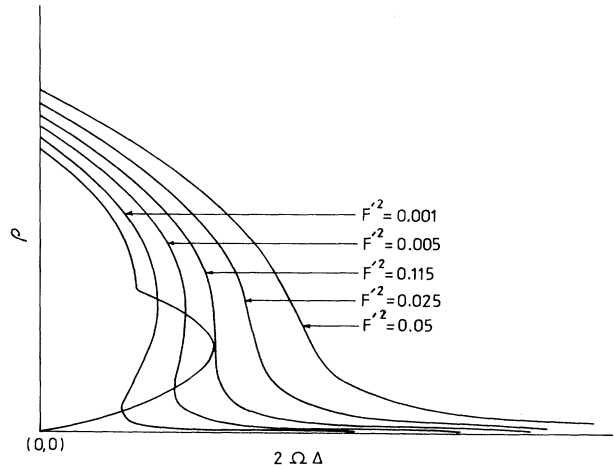


FIG. 1. Different zones of stability for different values of amplitude. ( $v = 1.0, A_2 = 1.25, A_4 = -3.0, A_6 = 1.5.$ )

### 2. Without the assumption of $\dot{x} = R(x)$

We now again analyze the regions of stability without the assumption  $\dot{x} = R(x)$ . This time the equation of motion is written as

$$\ddot{x} + \omega_0^2x + (v\dot{x} - A_4x^3 - A_6x^5) = F \cos(\Omega t). \tag{9}$$

As before we set

$$\begin{aligned} x &= a(t)\cos(\Omega t) + b(t)\sin(\Omega t) \\ &= r \cos(\Omega t + \phi), \end{aligned} \tag{10}$$

whence proceeding as before, we obtain

$$\begin{aligned} \frac{25}{64}A_6^2\rho^5 + \frac{15}{16\Omega^2}A_4A_6\rho^4 + \left[ \frac{9}{16\Omega^2}A_4^2 + \frac{5}{2}\frac{\Delta}{\Omega}A_6 \right]\rho^3 \\ + \frac{3\Delta}{\Omega}A_4\rho^2 + (4\Delta^2 + v^2)\rho = \left[ \frac{F}{\epsilon\Omega} \right]^2 = F_1, \end{aligned} \tag{11}$$

which is again a fifth-degree equation for  $\rho$  and quadratic in  $\Delta' = 2\Omega\Delta$ . An analysis similar to that of Sec. II A 1 can be done by considering a small variation from the singular values  $a_0$  and  $b_0$ , which leads to different zones of stability. Numerical analysis of this case is depicted in Figs. 2(a) and 2(b) for two sets of parameters.

In Figs. 1, 2(a), and 2(b) we have depicted the regions pertaining to center and saddle point for the parameter values  $A_2, A_4, A_6$ , and  $F$ . It may be observed readily that the system, with and without the ansatz  $\dot{x} = R(x)$ , behaves in a widely different manner. It appears therefore that the heteroclinic orbit obtained by Otwinowski, Paul, and Laidlaw<sup>4</sup> describes a completely different dynamics.

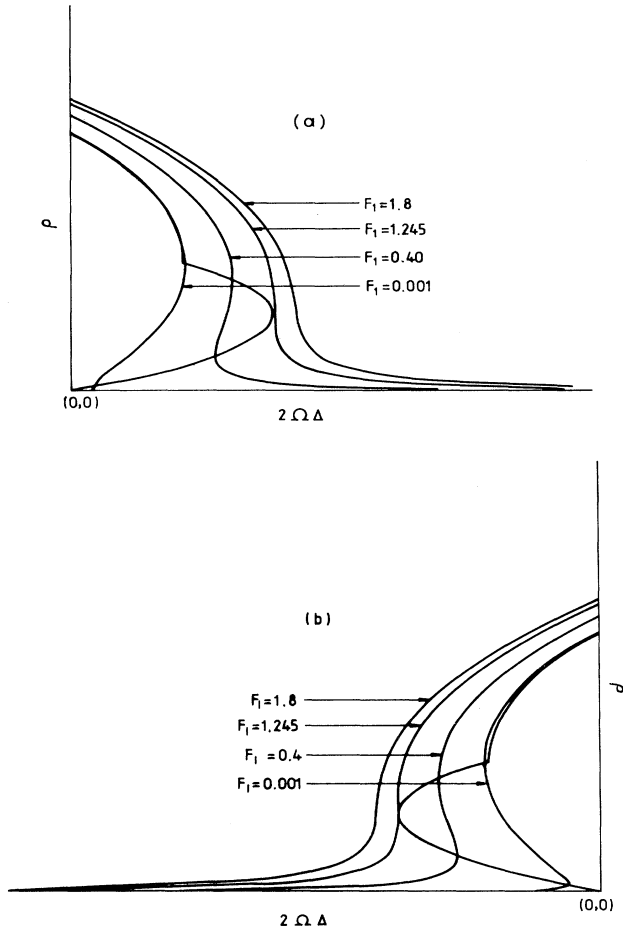


FIG. 2. (a) Figure showing different zones of stability for different values of amplitude. ( $v=1.0$ ,  $A_2=-1.0$ ,  $A_4=-3.0$ ,  $A_6=1.5$ ,  $\Omega=0.01$ .) (b) Figure showing different zones of stability for different values of amplitude. ( $v=1.0$ ,  $A_2=-1.0$ ,  $A_4=3.0$ ,  $A_6=-1.5$ ,  $\Omega=0.01$ .)

### B. Response curve

It is already known that the actual characteristics of the motion of such forced nonlinear oscillators are usually best described with the help of response curves. This was demonstrated by Bogoliubov and Mitropolsky<sup>5</sup> in 1961. The same procedure is adopted in the present case. The hysteresis-type phenomenon occurring in such nonlinear motion can very easily be understood with the help of such analysis. For our present situation we again start from

$$\ddot{x} + v\dot{x} + \omega_0^2 x + \epsilon(-A_4 x^3 - A_6 x^5) = 0. \quad (12)$$

This is the situation without the forcing term. We further assume that the solution is given as

$$x = r \cos(\omega t + \phi) + \epsilon x_1, \quad (13)$$

where the frequency  $\omega$  is near  $\omega_0$  and  $\omega = \omega_0 + \epsilon\omega_1$ . Substituting (13) in Eq. (12) and neglecting terms of  $O(\epsilon^2)$  we get

$$\omega_1 = \frac{1}{2\omega_0} \left( -\frac{5}{8} A_6 r^4 - \frac{3}{4} A_4 r^2 \right). \quad (14)$$

As is well known, the nonlinear oscillator can now be interpreted as a linear oscillator with the frequency-amplitude relation given by Eq. (14). It has now become a standard result of the linear theory for that of an oscillator with frequency  $\omega$  under a forcing  $F \cos(\Omega t)$

$$x = \frac{F \cos(\Omega t + \phi)}{[(\omega^2 - \Omega^2)^2 + v^2 \Omega^2]^{1/2}} \quad (15)$$

and by our assumption this must be equal to  $r \cos(\Omega t + \phi)$ . Now, if we are near the resonance region  $\Omega = \omega_0 + \epsilon\Delta$ , the above analysis entails

$$\left[ \frac{1}{2\omega_0} \left[ \frac{5A_6}{8} r^4 + \frac{3}{4} A_4 r^2 \right] + \Delta \right]^2 + \left[ \frac{v}{2\epsilon} \right]^2 = \frac{F^2}{4\omega_0^2 r^2 \epsilon^2} \quad (16)$$

which, in fact, is the required response curve. On the other hand, setting  $\partial\rho/\partial\Delta=0$ ,  $\rho=r^2$ , we obtain the skeleton curve

$$\Delta'' = (2\omega_0\Delta) = -\left( \frac{5}{8} A_6 \rho^2 + \frac{3}{4} A_4 \rho \right). \quad (17)$$

In Figs. 3(a) and 3(b) we have plotted the response curve and the skeleton curve for various values of  $F'^2 = (F/\epsilon)^2$  large and small, while the other parameters are restricted to two sets of values. According to the procedure mentioned in the general discussion by Bogoliubov and Mitropolsky<sup>5</sup> it would now be easy to ascertain the regions of stable and unstable motion from these diagrams. One has to sort out the regions of the curve along which  $\partial\rho/\partial\Delta''$  is greater than 0 or  $\partial\rho/\partial\Delta''$  is less than 0. The figures obtained fall in two basic categories. For higher values of  $F$ , we get Figs. 3(a) and 3(b) which are typical examples of hysteresis-type motion as had been observed in the case of the Duffing oscillator.<sup>5</sup> As the magnitude of frequency of the periodic forcing term increases or decreases, the amplitude of the oscillator moves along  $OA$  and then suddenly drops down to  $N$  and proceeds up to  $C$ , which on reduction of frequency moves back up to  $O'$  and suddenly jumps to  $B$ , thus forming the hysteresis loop. This type of motion, a jump had already been observed in the case of the Duffing oscillator<sup>5</sup> by Bogoliubov and Mitropolsky.

On the other hand, for smaller values of  $F$  we get the curves shown in Figs. 4(a) and 4(b), where the hysteresis-type motion is no longer visible; these figures now only depict the zones of stability of the motion. The response curve in the case with  $\dot{x} = R(x)$  has also been studied. In this situation a new phenomenon occurs. The portions of the curves  $OA$  and  $NA$  do not meet, and as may be seen from the analytic expression of  $\Delta$  in terms of  $\rho$ , they actually are asymptotic ( $\rho \rightarrow \infty$ ). Therefore the motion on either side of the skeleton curve is not connected to the other, and the hysteresis phenomenon is now absent. Thus it may be concluded that when the ansatz  $\dot{x} = R(x)$  is introduced following the methods used by Otwinowski, Paul, and Laidlaw,<sup>4</sup> the motion of the nonlinear oscillator is totally changed. Although consistency has been in-

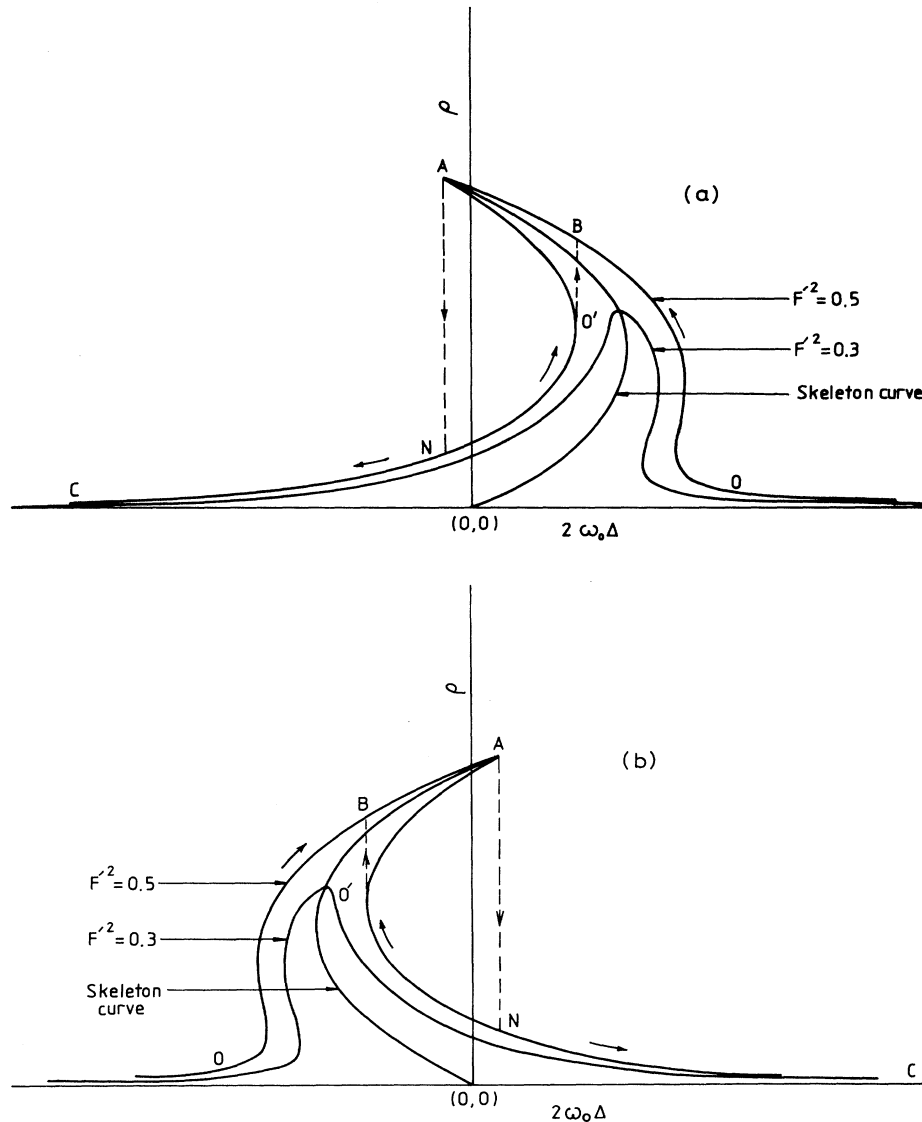


FIG. 3. (a) Hysteresis curves for different values of amplitude together with skeleton curve. ( $\nu = 1.0$ ,  $A_2 = -1.0$ ,  $A_4 = -3.0$ ,  $A_6 = 1.5$ .) (b) Hysteresis curves for different values of amplitude together with skeleton curve. ( $\nu = 1.0$ ,  $A_2 = -1.0$ ,  $A_4 = 3.0$ ,  $A_6 = -1.5$ .)

voked, the two types of motions represented are quite distinct. Even though heteroclinic orbits were obtained by Otwinowski, Paul, and Laidlaw,<sup>4</sup> yet it does not represent the actual damped motion given by Eq. (1). Lastly, the response function has been evaluated numerically by integrating Eq. (1) through the Runge-Kutta method, whence  $x$  is obtained at every instant of time. The response function is then defined by

$$R = \langle x^2 \rangle - \langle x \rangle^2, \quad (18)$$

where  $\langle \rangle$  denotes an average over a period  $T = 2\pi/\Omega$ . The corresponding result has been depicted in Figs. 5(a)–5(c). In Figs. 5(a) and 5(b), the response curve is seen to be quite similar to the one obtained analytically. On

the other hand, Fig. 5(c) shows that for the one obtained at the parameter values, period doubling has been obtained.

### C. Period doubling

The next important feature of the nonlinear system under consideration has been the phenomenon of period doubling, which may be deemed to be one of the most important routes to chaos. Such period doubling actually was observed to occur in the analytical procedure, which utilizes the properties of the Mathieu equation,<sup>6</sup> an approach adopted by earlier authors.<sup>6,7</sup>

Let us consider a small deviation  $\delta(t)$  from the solution

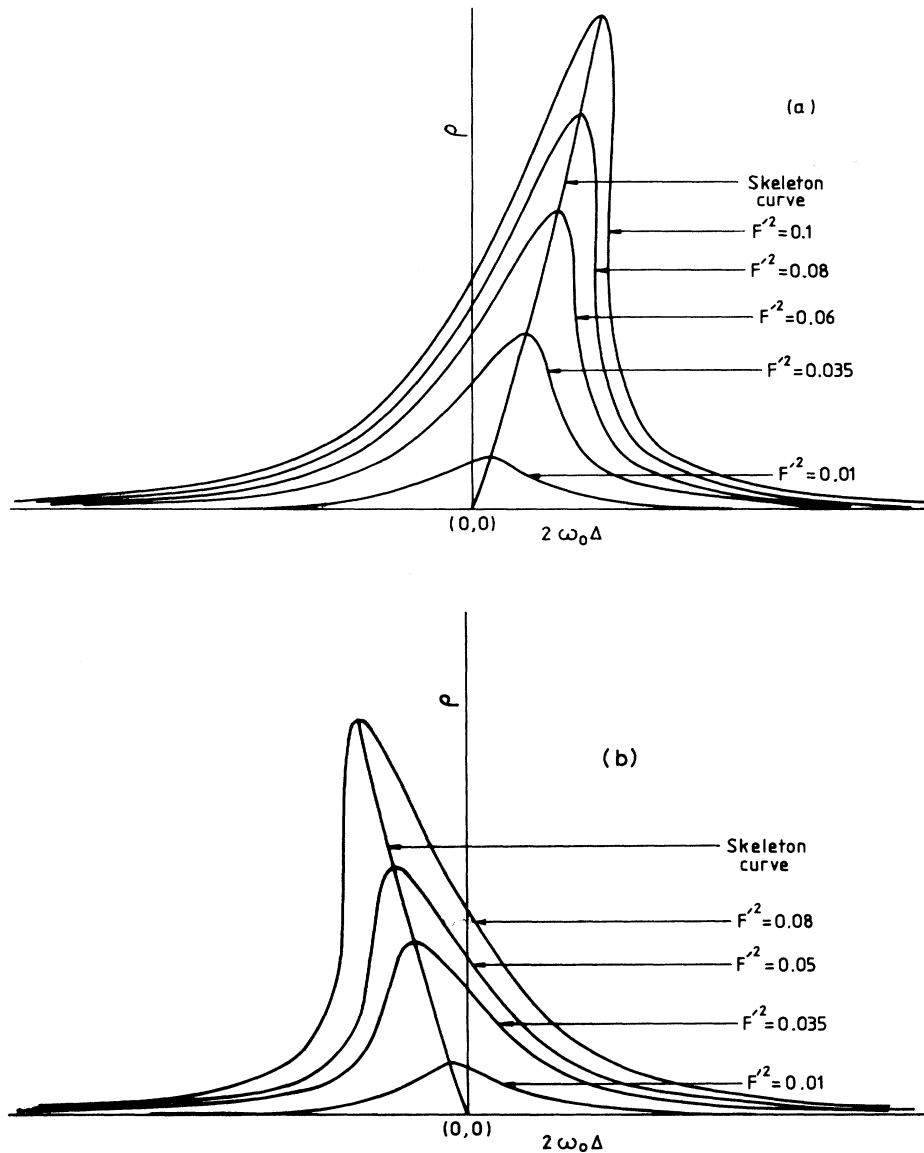


FIG. 4. (a) Response curves for different values of amplitude together with skeleton curve. ( $v=1.0, A_2=-1.0, A_4=-3.0, A_6=1.5.$ ) (b) Response curves for different values of amplitude together with skeleton curve. ( $v=1.0, A_2=-1.0, A_4=3.0, A_6=-1.5.$ )

discussed in Sec. II B. So we set

$$x = r \cos(\Omega t + \phi) + \delta(t), \tag{19}$$

whence by neglecting the contribution of higher-order harmonics we get the following equation for  $\delta(t)$ :

$$\frac{d^2\delta}{dt^2} + K \frac{d\delta}{dt} + [P + Q \cos(2\phi')] \delta = 0, \tag{20}$$

where

$$\phi' = \Omega t + \phi, \quad K = \frac{v}{\Omega}, \quad P = \frac{P'}{\Omega^2}, \quad Q = \frac{Q'}{\Omega^2}, \tag{21}$$

$P'$  and  $Q'$  are given by the following expressions;

$$\begin{aligned} P' &= -A_2 - \frac{3}{2}A_4r^2 - \frac{15}{8}A_6r^4, \\ Q' &= -\frac{3}{2}r^2A_4 - \frac{5}{2}A_6r^4. \end{aligned} \tag{22}$$

Equation (20) differs from the usual Mathieu equation due to the presence of the first-order derivative term, yet it can be analyzed according to the same procedure of Fourier analysis. Let us now substitute<sup>8</sup>

$$\delta(\phi') = \sum_{m=0}^{\infty} [A'_m \cos(m\phi') + B'_m \sin(m\phi')] \tag{23}$$

in Eq. (20), so that we get

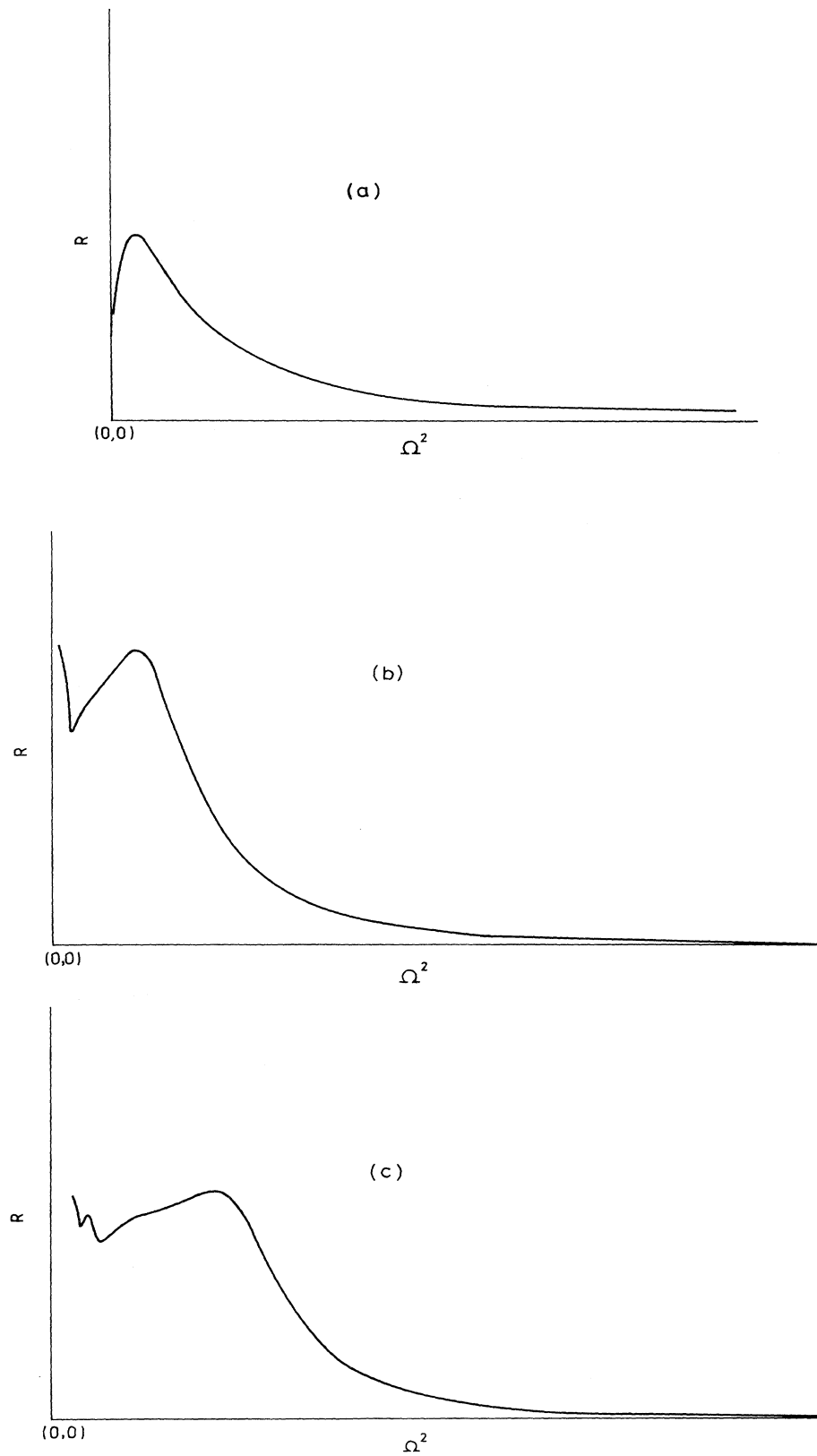


FIG. 5. (a) Numerically obtained response curve. ( $\nu = 1.0$ ,  $A_2 = -1.0$ ,  $A_4 = -3.0$ ,  $A_6 = 1.5$ ,  $F = 0.15$ .) (b) Numerically obtained response curve. ( $\nu = 1.0$ ,  $A_2 = -1.0$ ,  $A_4 = 3.0$ ,  $A_6 = -1.5$ ,  $F = 5.0$ .) (c) Numerically obtained response curve. ( $\nu = 1.0$ ,  $A_2 = -1.0$ ,  $A_4 = 3.0$ ,  $A_6 = -1.5$ ,  $F = 6.1$ .)

$$\sum_{m=0}^{\infty} [(P - m^2)A'_m + KmB'_m] \cos(m\phi') + \frac{Q}{2} \sum_{m=0}^{\infty} A'_m [\cos(m+2)\phi' + \cos(m-2)\phi']$$

$$+ \sum_{m=0}^{\infty} [(P - m^2)B'_m - KmA'_m] \sin(m\phi') + \frac{Q}{2} \sum_{m=0}^{\infty} B'_m [\sin(m+2)\phi' + \sin(m-2)\phi'] = 0. \quad (24)$$

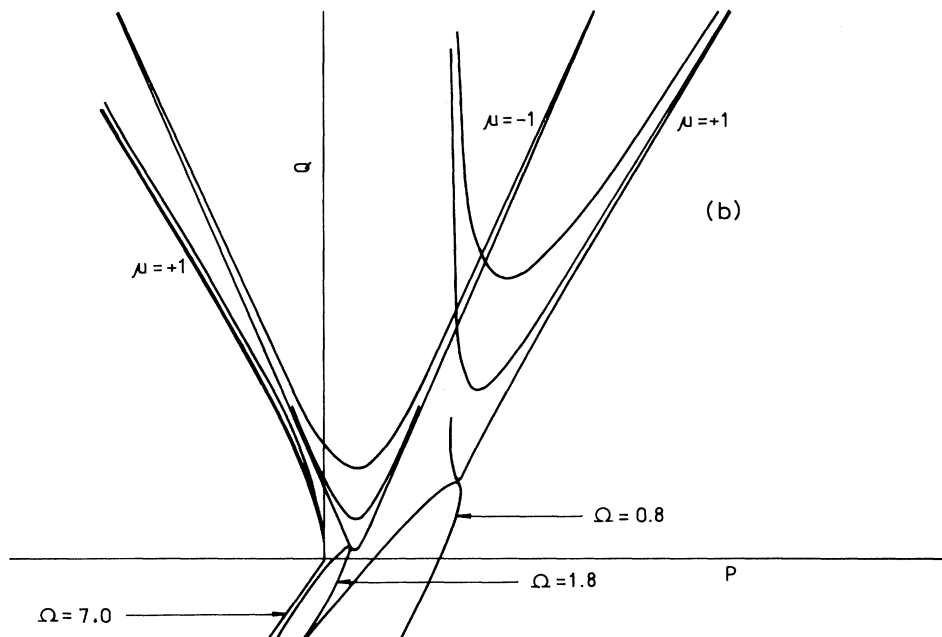
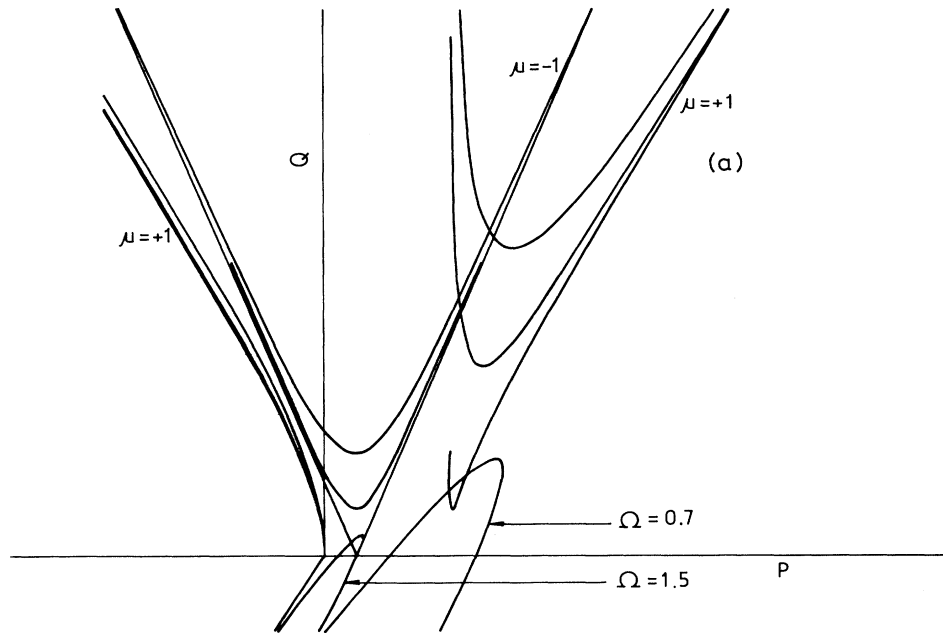


FIG. 6. (a) Zone boundaries and locus curve. ( $v = 1.0, A_2 = -1.0, A_4 = -3.0, A_6 = 1.5$ .) (b) Zone boundaries and locus curve. ( $v = 1.0, A_2 = -1.0, A_4 = -3.0, A_6 = 1.5$ .) (c) Zone boundaries and locus curve. ( $v = 1.0, A_2 = -1.0, A_4 = 3.0, A_6 = -1.5$ .)

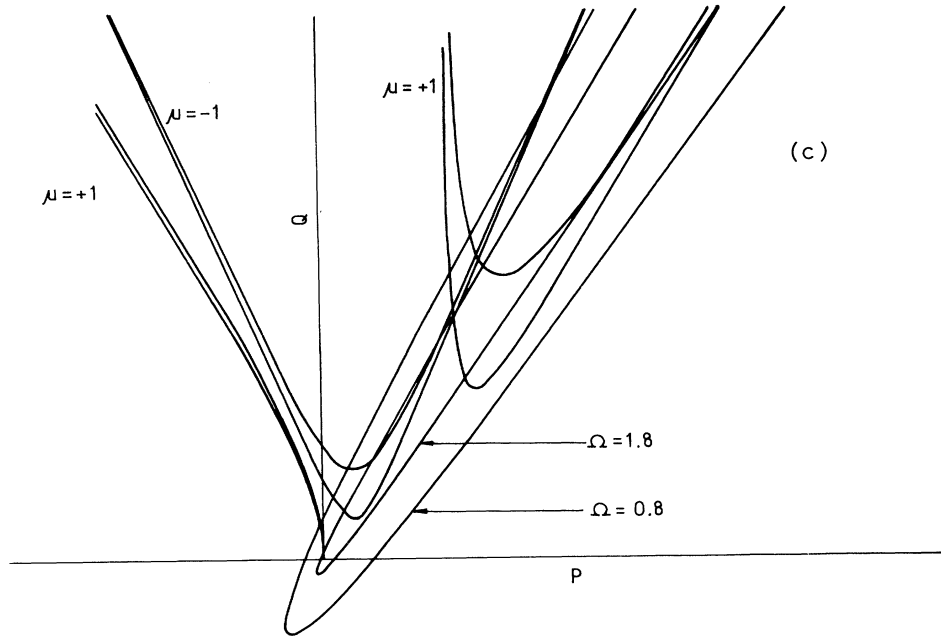


FIG. 6. (Continued).

From Eq. (24), considering terms up to second harmonics, we get the following expressions for even solutions:

The coefficient of  $\cos(0)$ , for period  $\pi$ , is

$$PA'_0 + \frac{Q}{2}A'_2 = 0. \tag{25}$$

The coefficient of  $\cos(\phi')$ , for period  $2\pi$ , is

$$(P-1)A'_1 + KB'_1 + \frac{Q}{2}(A'_1 + A'_3) = 0. \tag{26}$$

The coefficient of  $\cos(2\phi')$ , for period  $\pi$ , is

$$(P-4)A'_2 + 2KB'_2 + \frac{Q}{2}(2A'_0 + A'_4) = 0. \tag{27}$$

The expressions for odd solutions are as follows.

The coefficient of  $\sin(\phi')$ , for period  $2\pi$ , is

$$(P-1)B'_1 - KA'_1 + \frac{Q}{2}(B'_3 - B'_1) = 0. \tag{28}$$

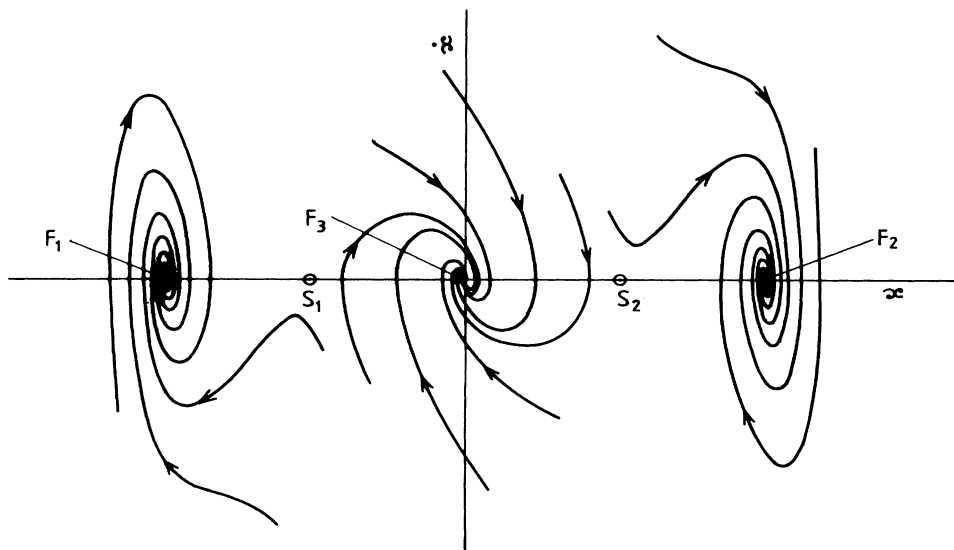


FIG. 7. Trajectories for the unperturbed damped system. ( $\nu=1.0, A_2=-1.0, A_4=3.0, A_6=-1.5.$ )  $F_1, F_2, F_3$ , stable focus points;  $S_1, S_2$ , saddle points.

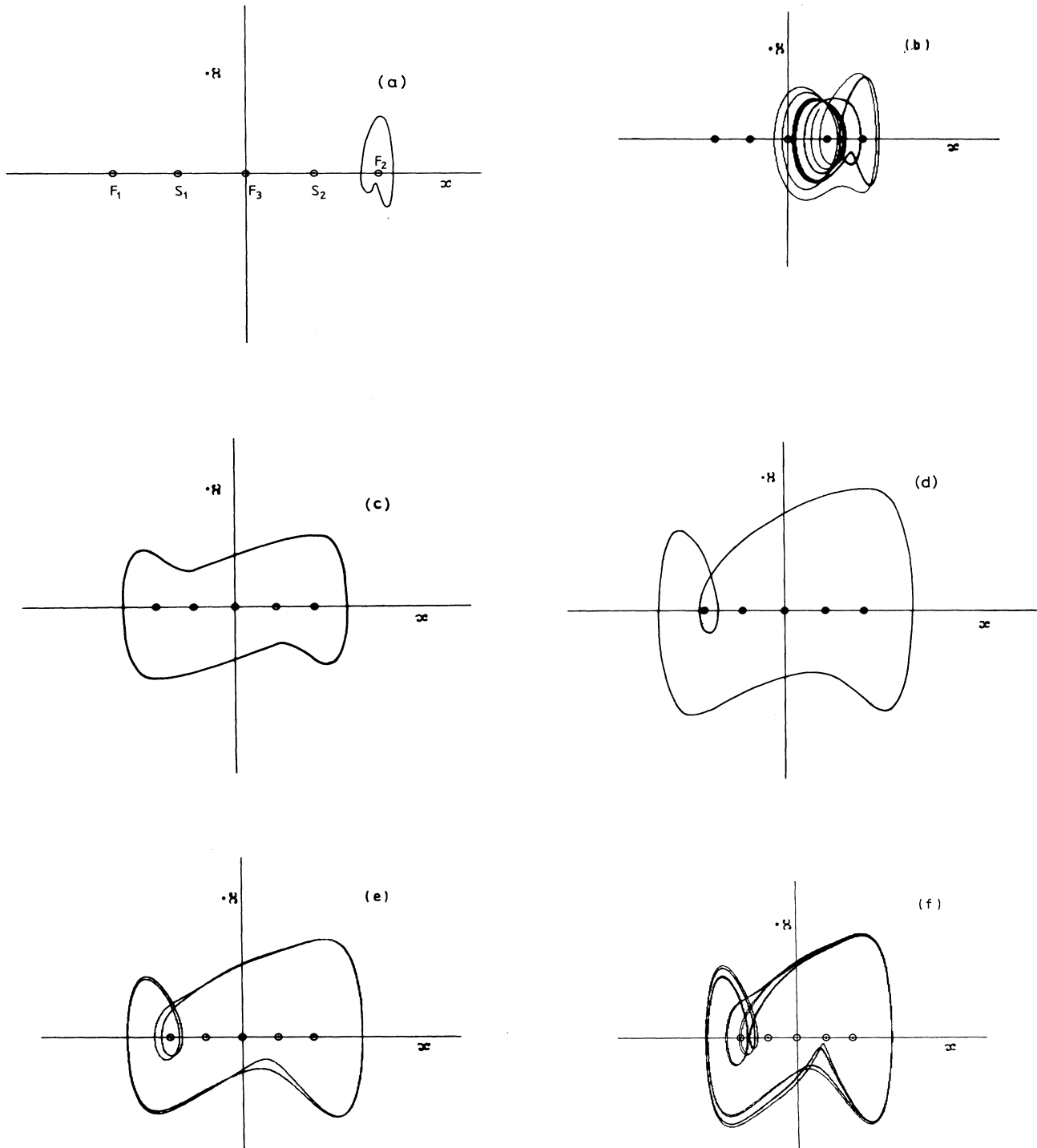


FIG. 8. (a) Phase diagram for the damped system under perturbation. ( $v=1.0$ ,  $A_2=-1.0$ ,  $A_4=3.0$ ,  $A_6=-1.5$ ,  $F=0.5$ ,  $\Omega=1.221$ .) (b) Phase diagram for the damped system under perturbation. ( $v=1.0$ ,  $A_2=-1.0$ ,  $A_4=3.0$ ,  $A_6=-1.5$ ,  $F=1.0$ ,  $\Omega=1.221$ .) (c) Phase diagram for the damped system under perturbation. ( $v=1.0$ ,  $A_2=-1.0$ ,  $A_4=3.0$ ,  $A_6=-1.5$ ,  $F=2.5$ ,  $\Omega=1.221$ .) (d) Phase diagram for the damped system under perturbation. ( $v=1.0$ ,  $A_2=-1.0$ ,  $A_4=3.0$ ,  $A_6=-1.5$ ,  $F=5.0$ ,  $\Omega=1.221$ .) (e) Phase diagram for the damped system under perturbation showing period doubling. ( $v=1.0$ ,  $A_2=-1.0$ ,  $A_4=3.0$ ,  $A_6=-1.5$ ,  $F=6.1$ ,  $\Omega=1.221$ .) (f) Phase diagram for the damped system under perturbation showing multiple periods. ( $v=1.0$ ,  $A_2=-1.0$ ,  $A_4=3.0$ ,  $A_6=-1.5$ ,  $F=6.81$ ,  $\Omega=1.221$ .) (g) Phase diagram for the damped system under perturbation. ( $v=1.0$ ,  $A_2=-1.0$ ,  $A_4=3.0$ ,  $A_6=-1.5$ ,  $F=7.0$ ,  $\Omega=1.221$ .)

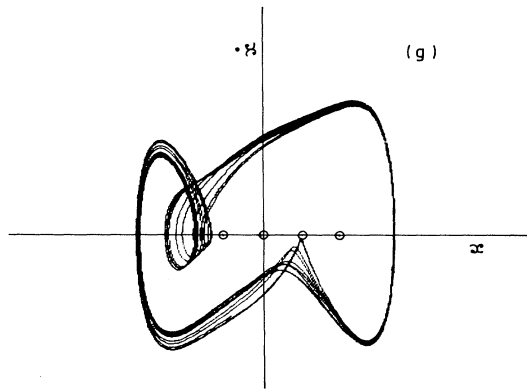


FIG. 8. (Continued).

The coefficient of  $\sin(2\phi')$ , for period  $\pi$ , is

$$(P-4)B'_2 - 2KA'_2 + \frac{Q}{2}B'_4 = 0. \tag{29}$$

So from the above relations we get the condition for the existence of a nontrivial solution  $\delta(t)$  with period  $\pi$  [that is, when the Floquet multiplier ( $\mu$ ) is +1]

$$Q^2 = 2P \left[ (P-4) + \frac{4K^2}{(P-4)} \right] \tag{30}$$

and the condition for the existence of a solution  $\delta(t)$  with period  $2\pi$  [that is, when the Floquet multiplier ( $\mu$ ) is -1] is

$$Q^2 = 4(P-1)^2 + 4K^2. \tag{31}$$

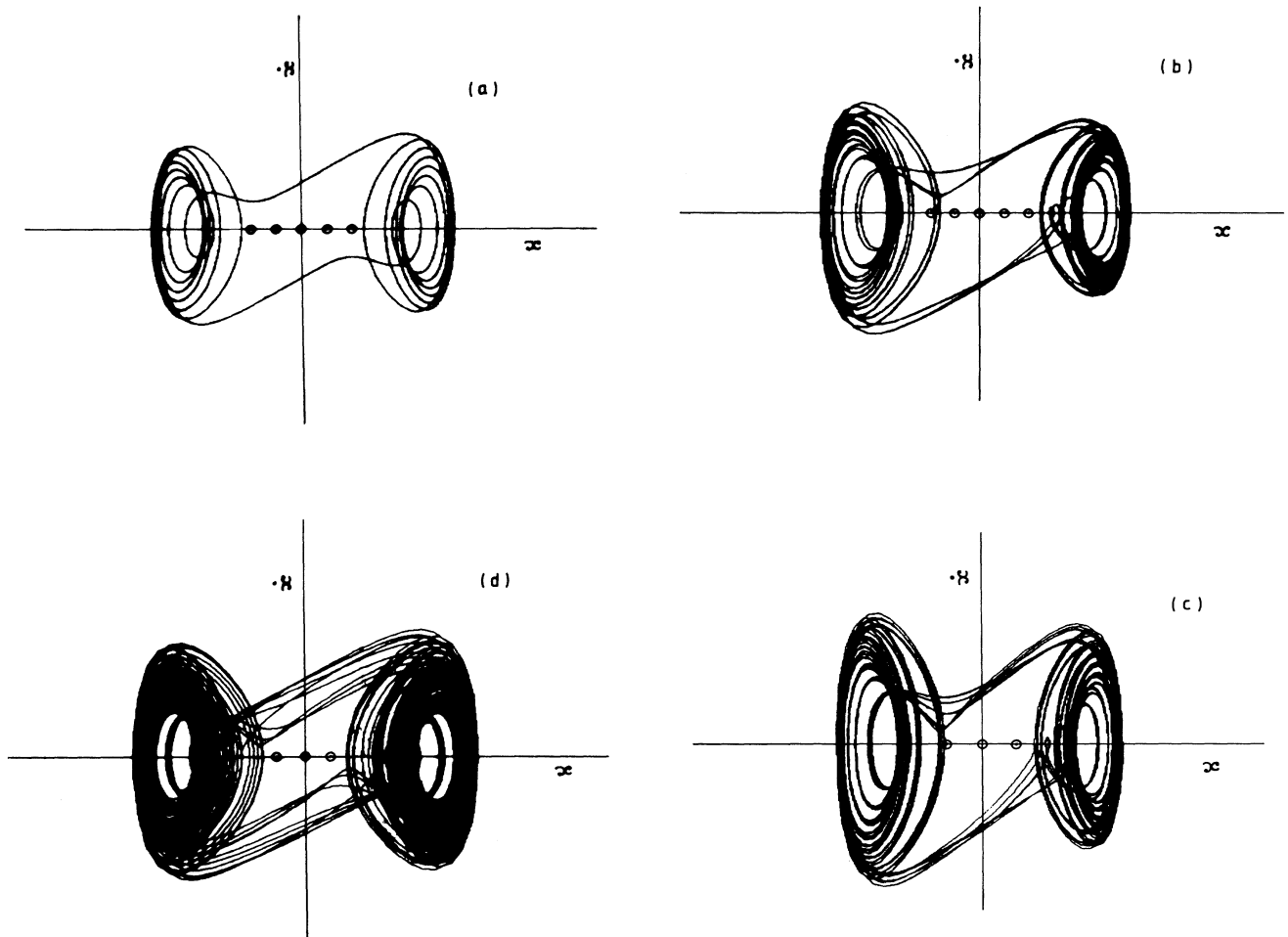


FIG. 9. (a) Phase diagram for the damped system under perturbation. ( $v=1.0, A_2=-1.0, A_4=3.0, A_6=-1.5, F=400.0, \Omega=1.221$ .) (b) Phase diagram for the damped system under perturbation. ( $v=1.0, A_2=-1.0, A_4=3.0, A_6=-1.5, F=456.0, \Omega=1.221$ .) (c) Phase diagram for the damped system under perturbation. ( $v=1.0, A_2=-1.0, A_4=3.0, A_6=-1.5, F=458.51, \Omega=1.221$ .) (d) Phase diagram for the damped system under perturbation. ( $v=1.0, A_2=-1.0, A_4=3.0, A_6=-1.5, F=480.0, \Omega=1.221$ .)

Lastly, the expression for  $P$  and  $Q$  implies a relation between them for all values of  $r$  (which we call the locus curve), and such a relation may be written as

$$\begin{aligned} \frac{9}{16}\Omega^4 Q^2 + MQ + N &= 0, \\ M &= \frac{9A_4^2}{40A_6}\Omega^2 - \frac{3}{2}A_2\Omega^2 - \frac{3}{2}P\Omega^4, \\ N &= P^2\Omega^4 + A_2^2 + 2\Omega^2 A_2 P - \frac{9A_4^2}{40A_6}P\Omega^2 - \frac{9A_4^2}{4A_6}A_2. \end{aligned} \quad (32)$$

In Figs. 6(a), 6(b), and 6(c) we have plotted Eqs. (30), (31),

$$(x, \dot{x}) = (0, 0), (\sqrt{\phi_+}, 0), (\sqrt{\phi_-}, 0), (-\sqrt{\phi_+}, 0), (-\sqrt{\phi_-}, 0),$$

with

$$\phi_{\pm} = \frac{1}{2A_6} [-A_4 \pm (A_4^2 - 2A_6 A_2)^{1/2}].$$

If we integrate Eq. (1) with the help of the fourth-order Runge-Kutta method taking initial values near each of these points, the behavior of these fixed points would become understandable. In case the parameter set assumes a different value, the corresponding fixed points reduce in number, two of them becoming imaginary. The nature of these fixed points has already been depicted in Fig. 7. It is seen that (0,0) is a stable focus point, two on the left and right of it (near to it) are saddle points while the extreme two are stable focus points. Now, if the periodic perturbation is introduced and the equation is again numerically integrated for various values of  $F$ , an interesting event takes place. When  $F$  is small (say, of the order of 0.5) the phase-space trajectory upon interaction does not leave the vicinity of the zone of the fixed point, close to which the initial value has been chosen. Now, if  $F$  is increased to say 1.0, and the trajectory is plotted again, it encompasses the fixed points on one side of the  $x$  axis. These are shown in Figs. 8(a) and 8(b). Further, if  $F$  is increased to 2.5 and 5.0, the phase diagram becomes as shown in Figs. 8(c) and 8(d). The trajectory appears to roam from one side to the other and comes back again, completing one periodic orbit. If  $F$  is again increased to 6.1, the period doubling is clearly observed as has been shown in Fig. 8(e). Higher-order trajectories are shown in Fig. 8(f) and 8(g) due to further increases in the value of  $F$  (6.81 and 7.0). Now when  $F=7.0$ , we observe a

and (32), respectively. It is clearly seen that they give the region in the  $P$ - $Q$  plane for the phenomena of period doubling, bifurcation, and hysteresis. These figures also very clearly show the positions of intersection<sup>9-11</sup> of Eqs. (30) and (31), with (32).

#### D. Global phase-space analysis

Since all the analytic computations presented above involve some degree of approximation, we now try to support our previous inferences by attempting some direct numerical analysis in the phase space. Our Eq. (1) has five fixed points given as

chaotic-type motion from the wandering of the orbits as has been shown in Fig. 8(g). But with a further change in the value of  $F$ , say when it is set to be equal to some other higher value, single closed orbits again appear in the phase-space diagram. This phenomenon is an indication of the appearance of the window in the chaotic regime, which is a common property of all period-doubling bifurcations. We have checked that at  $F=400.0$  the single orbit again appears [see Fig. 9(a)] and the process repeats until again chaos appears [see Figs. 9(b), 9(c), and 9(d)].

### III. DISCUSSION

In our above analysis we have made a detailed study in regard to the behavior of the nonlinear oscillator with higher-order nonlinearity, and under a periodic forcing term. Both analytical and numerical methods are adopted. The period doubling, stability, and response of the system as observed in the analytical treatment are corroborated by the numerical analysis performed. An important outcome of our analysis is that the system shows widely different behavior with or without the ansatz  $\dot{x} = R(x)$ .

#### ACKNOWLEDGMENTS

One of the authors (M.D.) is grateful to the University Grants Commission (Government of India) for financial support through the Fifth Plan Development Scheme.

<sup>1</sup>B. H. Huberman and J. P. Crutchfield, *Phys. Rev. Lett.* **93**, 1743 (1979); B. L. Hao and S. Y. Zhang, *Phys. Lett.* **87A**, 267 (1982).

<sup>2</sup>K. L. Liu and K. Young, *J. Math. Phys.* **27**, 502 (1986).

<sup>3</sup>R. E. Mickens, *An Introduction to Nonlinear Oscillations* (Cam-

bridge University Press, Cambridge, 1981).

<sup>4</sup>M. Otwinowski, R. Paul, W. G. Laidlaw, *Phys. Lett. A* **128**, 483 (1988).

<sup>5</sup>N. N. Bogoliubov and Y. A. Mitropolsky, *Asymptotic Methods in the Theory of Nonlinear Oscillations* (Gordan and Breach,

- New York, 1961).
- <sup>6</sup>T. Kapitaniak, *Phys. Lett. A* **144**, 322 (1990).
- <sup>7</sup>J. C. Huang, Y. H. Kao, C. S. Wang, and Y. S. Gou, *Phys. Lett. A* **136**, 131 (1989).
- <sup>8</sup>*Handbook of Mathematical Functions*, edited by M. Abramowitz and I. A. Stegun (Dover, New York, 1964).
- <sup>9</sup>T. Kapitaniak, *Chaos in Systems with Noise* (World Scientific, Singapore, 1988).
- <sup>10</sup>W. Szemplinska Stupnicka and J. Bajkowski, *Int. J. Non-Linear Mech.* **21**, 401 (1986).
- <sup>11</sup>A. Yamaguchi, H. Fujisaka, and M. Inoue, *Phys. Lett. A* **135**, 320 (1989).